

TRAFFIC SURVEILLANCE USING GABOR FILTER BANK AND KALMAN PREDICTOR

Mehmet Celenk¹, James Graham¹ and Santosh Singh²

¹*School of Electrical Engineering and Computer Science, Ohio University, Athens, OH 45701, USA*

²*Corporate Technology-India, Siemens Information Systems Ltd., Bangalore, India*

Keywords: Traffic surveillance, Gabor-filter bank, motion detection, non-linear Kalman filtering, scene prediction.

Abstract: This paper builds upon our earlier work by applying an optimized version of our non-linear scene prediction method to traffic surveillance video. As previously, a Gabor-filter bank has been selected as a primary detector for any changes in a given image sequence. The detected ROI (region of interest) in arbitrary motion is fed to a non-linear Kalman filter for predicting the next scene in time-varying video, which is subject to prediction error invalidation. Potential applications of this research are mainly in the areas of traffic control and monitoring, traffic flow surveillance, and MPEG video-compression. The reported experimental results show improved performance over the non-linear Kalman filtering based scene prediction results in our previous work. The low least mean square error (LMSE), on the average of about 2 to 3 % remains close to the average reported in our earlier work, however, the fluctuations in error have disappeared, proving the reliability of the approach to traffic-motion prediction.

1 INTRODUCTION

Over the last decade, the prediction of 2-D or 3-D scenes and the changes therein has become an increasingly popular research area (e.g., Kim and Woods (1998), Irani and Anandan (1998), Hoover et al. (2003), and Sawhney, et al. (2003)). This is due to its potential applications in unmanned navigation and guidance, surveillance, tracking, MPEG video compression, virtual world simulation, multimedia networking, animation, search and rescue. Two popular tools for these endeavors are the Kalman and Gabor filters. The Kalman filter (KF) is one of the most widely used methods for tracking and estimation because of its simplicity, optimality, tractability and robustness as reported in Roumeliotis and Bekey (2000a and 2000b) and Dorfmueller-Ulhaas (2003). In this study, we predict the changes in an arbitrary scene setting using a Kalman predictor. However, a direct use of the Kalman filter with a nonlinear system can be difficult. An effective method for alleviating nonlinearity is to use an extended Kalman filter (EKF) (Sorenson, 1985) as an estimator by linearizing all the nonlinear parameters in a nonlinear system (Julier and Uhlmann, 1987). The

Gabor filter (Theodoridis and Koutroumbas, 2006) has been proven to be useful for filtering based on texture differences within an image and is used in areas such as texture segmentation, document analysis, edge detection, retina identification, fingerprint processing, and image coding and representation. An example is Macenko *et al.*'s work (2007), which provides both a good explanation of the approach to using Gabor filtering and a highly relevant practical application in lesion detection within the brain. In this work, the prediction of frame to frame movement of the selected ROI in a given traffic image sequence is carried out by using a bank of Gabor filters to determine the region of interest (ROI), followed by the application of a nonlinear Kalman filter to the ROI to predict movement. Many other traffic surveillance and prediction methods have been proposed and implemented (e.g., (Huang and Russell, 1998), (Koller, et al., 1994), (Bramberger, et al., 2004), (Wang, et al., 2006), (Cheung, et al. 2005), (Celenk *et al.*, 2007a and 2007b). The work presented by Maire and Kamath (2005) is similar to ours in the respect that the goal is to track traffic; however, our approach uses a more robust ROI detection method with the use of Gabor filtering to capture shapes via texture difference and is not normally applied to an

estimation problem such as this one. Kalman filtering is not typically used in image prediction or paired with Gabor filtering as claimed to be one of the objectives herein. Furthermore, our Kalman predictor is able to adjust its prediction results as the input scene domain changes while the dual Kalman filtering method presented by Roumeliotis and Bekey (2000a), for example, makes use of a scene-domain model (i.e., no adaptability). The following sections describe the overall approach, experiments, and results obtained. Conclusions and future study are given at the end.

2 DESCRIPTION OF APPROACH

This paper takes the approach described in our earlier work (2007b) toward the scene prediction problem by using both Kalman and Gabor based filtering. Prediction of an entire image is not necessarily useful, desired, or even practical. Because of this, Gabor filtering helps determine a ROI in which to generate prediction results. The basic algorithm flow is shown in Figure 1.

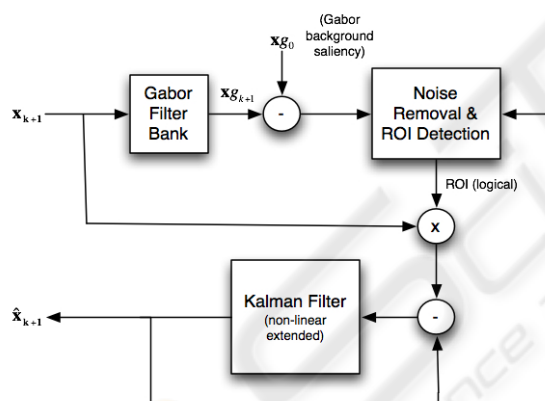


Figure 1: Algorithm flowchart.

Here, the current frame is fed to a Gabor filter bank which calculates the output images for a series of Gabor filters with varying orientations. The filter bank will cover the spatial-frequency space and capture the essential shape information. Gabor output images are employed to generate a combined saliency map. Moving object bounding boxes are created with the saliency image and previous error results from the Kalman filter. Overlapping boundary boxes are combined and boxes common to both are used to determine the logical ROI (region of interest). The ROI's relevant portion of the image is passed onto the extended Kalman filter.

3 EXPERIMENTAL RESULTS

A pair of data sets is used in experimentation from the Institute for Algorithms and Cognitive Systems of Karlsruhe University's traffic image sequence database, specifically, the Taxi sequence and the Rheinhafen sequence. The Taxi sequence was chosen for its relative simplicity, while the Rheinhafen sequence was chosen for its multiple trackable vehicles and more "normal" imagery. It is normal in the sense that there are a fair number of detection errors. Images provided in the databases are in 2-D intensity format. Since depth information is not provided, the Kalman filter models pixel intensity. The 2-D scene data used for this experiment is from a static surveillance camera, meaning the camera's position is fixed. In the collected images, only the scene contents move while the camera remains stationary. The Taxi and Rheinhafen images have been converted into JPEG images with resolutions of 256x191 and 688x565, respectively. Figure 2 shows a pair of example images from the selected databases depicted the scenes from which they were acquired.



Figure 2: Scenes from Taxi and Rheinhafen databases.

In our implementation, we follow the same discrete formulation of the Gabor filter as Macenko[11], which specifies the Gabor filter variables to be $S_x = 1$, $S_y = 1$, and $\theta = \{0, \pi/4, \dots, \pi, \dots, 7\pi/4\}$. Eight different orientations for the Gabor bank are adapted since more would not provide any significant improvement and fewer would likely not discern enough about the image. Upon passing the image through the filter bank a combined saliency image is created. The saliency image has the background saliency image subtracted to leave only the correct region of interest (ROI). The resulting ROI image is then passed through a noise reduction and blocking filter to remove "specks" which results from small background changes and to "block out" the ROI to give it slightly better coverage. Figure 3 illustrate the process of determining the ROI. Image (a) shows the Gabor saliency image for the background, while image (b) shows the Gabor

saliency for the current frame. The next image, image (c), depicts the result of the noise removal and black and white conversion of the previous image. The final image, (d), shows the results of “boxing” the ROI. To generate this last image, the ROI is combined with the previous cycle’s Kalman error to generate a number of boundary boxes. These boxes are then combined or removed as needed depending on their relative positions to each other and their relationship with the known ROI. In the image below the green regions are those associated with the ROI, while the red regions are those that have been “thrown away.” The blocking ensures that most of the pixels immediately surrounding the region of interest get included in the Kalman filter estimations and has the secondary effect of allowing actual tracking of moving objects.

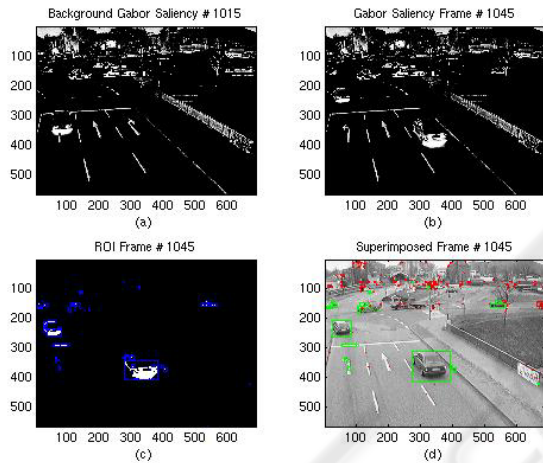


Figure 3: Gabor filter results for frame #1045 of the Rheinhafen database.

Next, the superimposed frame containing the selected ROI (the green boxes) is passed on to the Kalman filter. The Kalman filter is then applied to the region of interest. To alleviate computational time issues and better handle the uneven lines of the ROI, the filter is run on 3x3 subsets or blocks of the total image. A 3x3 pixel filter is run for each frame, and the predicted results are then combined to create a full scene image array. In experimentation, the pixel noise value (pn_{ij}) is assumed to be zero, and velocity is not taken into account. The state transition matrix ϕ_k is adjusted for a 3x3 window based Kalman filter realization as a 27x27 matrix given by

$$\phi_k = \begin{bmatrix} I & I & I \\ 0 & I & I \\ 0 & 0 & I \end{bmatrix}$$

where I is a 9x9 identity matrix and θ is a 9x9 zero matrix. The noise variance (σ_{ij}^2) is considered as white Gaussian noise with a value of 0.25. In our experiment the pixel noise (pn_{ij}) is assumed to be 0, and the velocity noise (vn_{ij}) is taken to be 1 m/s. The prediction error, e , for the described method is calculated between the observed (f_{k+1}) and predicted (\hat{f}_{k+1}) images following the k^{th} iteration in the least mean square sense (LMSE). The LMSE computation is carried out over the whole image frame of size $M \times N$ at pixel level (i, j) using

$$e = \sqrt{\frac{1}{M \cdot N} \sum \sum (\hat{f}_{k+1}(i, j) - f_{k+1}(i, j))^2} \quad (1)$$

Figure 4 gives an example of the prediction results for the same frame of the Rheinhafen database shown above. The measured frames represent the actual frame, while the predicted frame is the frame predicted from the previous cycle. Discrepancies tend to occur because the section of the image that they are associated with is not part of the region of interest but instead part of the background of their particular frame and, thus, not tracked.

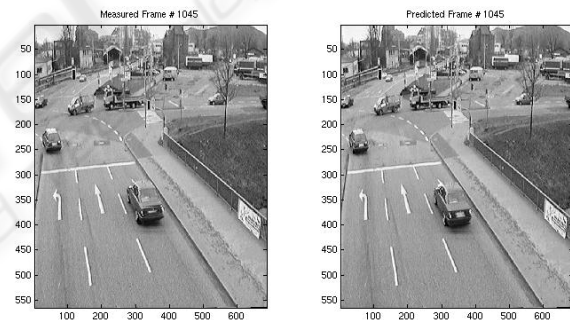


Figure 4: Prediction results.

Figures 5 and 6 present the LMSE error results for all 41 frames of the Taxi database and frames 1015 to 1055 of the Rheinhafen database.

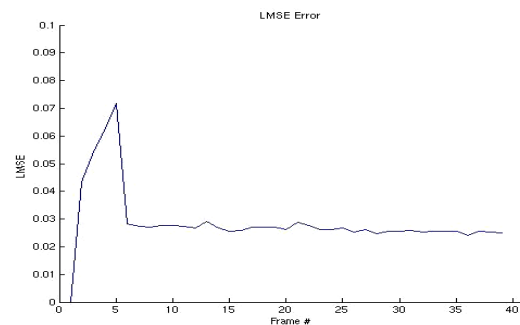


Figure 5: LMSE results for the Taxi database.

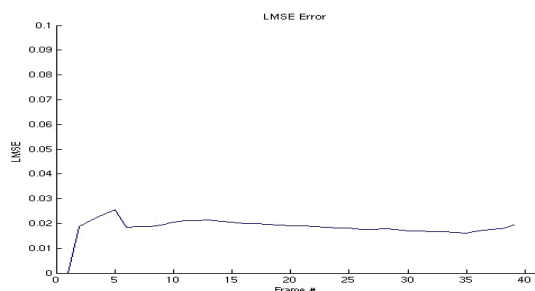


Figure 6: LMSE results for the Rheinhafen database.

4 CONCLUSIONS

This work has the objective of predicting mobile objects in video scenes as the camera or sensory device mounted on a platform remains stationary. Unlike existing target detection and tracking research, it makes use of Gabor filtering (and boundary box method) to select the ROI and a nonlinear extended Kalman filtering as a feedback mechanism to accurately track the moving targets and predict their locations ahead of time. The reported experimental results demonstrate that the nonlinear Kalman filtering based scene prediction performs well and can accurately estimate the next frames in images to a certain degree of accuracy. The low LMSE error measurement of the nonlinear filter prediction, on the average of about 2 to 3 %, proves the reliability and robustness of this approach to time-varying image data processing. The presented results are reasonably low in error for low-cost visible and IR camera applications [17, 21]. Potential areas for future research lie in devising an ROI tracking mechanism in lieu of semantic information and improvements to the Kalman filtering algorithm to adjust itself for high-level visual clues. The magnitude of the prediction error involving initial frames indicates that further work is needed for the performance improvement.

REFERENCES

- Bramberger, M., et al. (2004) Real-time video analysis on an embedded smart camera for traffic surveillance. *In Proc. of 10th IEEE RTAS Symp.*, pp. 174-181.
- Celenk, M., et al., (2007a) A Kalman filtering approach to 3-D IR scene prediction using single-camera range video," in *Proc. IEEE ICIP, San Antonio, TX*.
- Celenk, M., et al. (2007b) Non-linear IR scene prediction for range video surveillance. *In 4th Joint IEEE Int. Workshop on OTCBVS'0*), Minneapolis, MN
- Cheung, S.Y., et al., (2005) Traffic surveillance with wireless magnetic sensors. *In Proc. 12th ITS World Congress, San Francisco, Nov. 2005*.
- Dorfmueller-Ulhaas, K. (2003) *Robust optical user motion tracking using a Kalman filter*. Technical Report. University of Augsburg, May 2003.
- Hoover A., et al., (2003) Egomotion estimation of a range camera using the space envelope. *IEEE-TSMCB*, 33(4), pp. 717-721.
- Huang, T. and Russell, S. (1998) Object identification: A Bayesian analysis with application to traffic surveillance. *Artificial Intel.*, 103(1), pp. 77-93.
- Institute for Algorithms and Cognitive Systems, Image Sequence Server, Karlsruhe University, <http://i21www.ira.uka.de/image_sequences>.
- Irani, M., and Anandan P. (1998) A unified approach to moving object detection in 2D and 3D scenes. *IEEE-T-PAMI*, 20(6), pp. 577-589.
- Julier, S. J. and Uhlmann, J. K. (1997) A new extension of the Kalman filter to nonlinear systems. *In Proc. of AeroSense*, Orlando, FL
- Kim, J. and Woods, J.W. (1998) 3-D Kalman filter for image motion estimation. *IEEE-T-IP*, 7(1), pp. 42-52.
- Koller, D., et al., (1994) Towards robust automatic traffic scene analysis in real-time. *In Proc. IAPR*.
- Macenko, M., et al., (2007) Lesion detection using Gabor-based saliency field mapping. *Medical Imaging 2007, Proc. SPIE Vol. 6512*, Feb. 17-24, San Diego, CA.
- Maire, M. and Kamath, C. (2005) Tracking Vehicles in Traffic Surveillance Video. Lawrence Livermore National Lab., Technical Report UCRL-TR-214595.
- Roumeliotis, S. I. and Bekey, G. A. (2000a) SEGMENTS: A Layered, Dual-Kalman filter Algorithm for Indoor Feature Extraction. *Proc. IROS 2000*, pp. 454-461.
- Roumeliotis, S. I. and Bekey, G. A. (2000b) Bayesian estimation and Kalman filtering: A unified framework for Mobile Robot Localization. *Proc. IEEE Conf. Robotics and Autom.*, pp. 2985-2992.
- Sawhney, H.S, et al., (2000) Independent motion detection in 3D scenes. *IEEE-T-PAMI*, 22(10), pp. 1191-1199.
- Sorenson, H. W. (1985) *Kalman Filtering: theory and application*. IEEE Press, 1985.
- Theodoridis, S. and Koutroumbas, K. (2006) *Pattern Recognition*. 3rd ed., Academic Press.
- Wang, Y., et al. (2006) Renaissance: A real-time freeway network traffic surveillance tool. *In IEEE ITSC '06*.